NeuroD Factors Discriminate Mineralocorticoid From Glucocorticoid Receptor DNA Binding in the Male Rat Brain

Lisa T.C.M. van Weert,[1,4,5] Jacobus C. Buurstede,[1] Ahmed Mahfouz,[2,6] Pamela S.M. Braakhuis,[1] J. Annelies E. Polman,[7] Hetty C.M. Sips,[1] Benno Roozendaal,[4,5] Judit Balog,[3] E. Ronald de Kloet,[1,7] Nicole A. Datson,[7] and Onno C. Meijer[1]

[1]Department of Medicine, Division of Endocrinology, Leiden University Medical Center, 2300 RC, Leiden, The Netherlands; [2]Department of Radiology, Division of Image Processing, Leiden University Medical Center, 2300 RC, Leiden, The Netherlands; [3]Department of Human Genetics, Leiden University Medical Center, 2300 RC, Leiden, The Netherlands; [4]Department of Cognitive Neuroscience, Radboud University Medical Center, 6500 HB, Nijmegen, The Netherlands; [5]Donders Institute for Brain, Cognition, and Behaviour, Radboud University, 6525 EN, Nijmegen, The Netherlands; [6]Delft Bioinformatics Laboratory, Delft University of Technology, 2628 CD, Delft, The Netherlands; and [7]Division of Medical Pharmacology, Leiden/Amsterdam Center for Drug Research, 2300 RC, Leiden, The Netherlands

In the limbic brain, mineralocorticoid receptors (MRs) and glucocorticoid receptors (GRs) both function as receptors for the naturally occurring glucocorticoids (corticosterone/cortisol) but mediate distinct effects on cellular physiology via transcriptional mechanisms. The transcriptional basis for specificity of these MR- vs GR-mediated effects is unknown. To address this conundrum, we have identified the extent of MR/GR DNA-binding selectivity in the rat hippocampus using chromatin immunoprecipitation followed by sequencing. We found 918 and 1450 nonoverlapping binding sites for MR and GR, respectively. Furthermore, 475 loci were co-occupied by MR and GR. *De novo* motif analysis resulted in a similar binding motif for both receptors at 100% of the target loci, which matched the known glucocorticoid response element (GRE). In addition, the Atoh/NeuroD consensus sequence was found in co-occurrence with all MR-specific binding sites but was absent for GR-specific or MR-GR overlapping sites. Basic helix-loop-helix family members Neurod1, Neurod2, and Neurod6 showed hippocampal expression and were hypothesized to bind the Atoh motif. Neurod2 was detected at rat hippocampal MR binding sites but not at GR-exclusive sites. All three NeuroD transcription factors acted as DNA-binding–dependent coactivators for both MR and GR in reporter assays in heterologous HEK293 cells, likely via indirect interactions with the receptors. In conclusion, a NeuroD family member binding to an additional motif near the GRE seems to drive specificity for MR over GR binding at hippocampal binding sites. (***Endocrinology*** **158: 1511–1522, 2017)**

The endogenous glucocorticoid hormone of the rat, corticosterone, has a profound action on the brain. This action is mediated in a complementary manner by mineralocorticoid receptors (MRs) and glucocorticoid receptors (GRs), which are unevenly distributed over the brain, but coexpressed in abundance in the hippocampus (1). The high-affinity MRs are already substantially occupied with low corticosterone levels (2). In the initial response to stress, these MRs play a crucial role in retrieval of stressful information and the selection of an appropriate coping response (3–5). In contrast, the lower-affinity GRs become activated only at higher corticosterone levels, around the peak of the circadian rhythm and during a stress response. GR activation promotes memory storage of the stressful experience (6, 7) and behavioral adaptation and recovery (1, 8).

ISSN Print 0013-7227 ISSN Online 1945-7170
Printed in USA

Received 15 June 2016. Accepted 18 January 2017.
First Published Online 24 January 2017

Abbreviations: AF, activator function; AME, analysis of motif enrichment; bHLH, basic helix-loop-helix; CA, cornu ammonis; cDNA, complementary DNA; ChIP-seq, chromatin immunoprecipitation sequencing; DBD, DNA-binding domain; DG, dentate gyrus; GR, glucocorticoid receptor; GRE, glucocorticoid response element; IgG, control immunoglobulin G; LBD, ligand-binding domain; MACS, model-based analysis of chromatin immunoprecipitation sequencing; MR, mineralocorticoid receptor; NP, Nonidet P; qPCR, quantitative polymerase chain reaction; RT, reverse transcription.

Much progress has been made in understanding the cellular mechanism of these coordinated MR–GR–mediated actions of corticosterone (9). Many of the effects depend on the transcriptional activity of the receptors. MR-mediated actions generally raise excitability in the hippocampus. In the most ventral part of the hippocampus, corticosterone prolongs excitability via GR, providing an extended period for encoding of new information. In the dorsal pyramidal cells, GR-mediated actions oppose those mediated by MR (10). That these MR- and GR-mediated effects of corticosterone are sometimes overlapping and, in other processes, are distinct is remarkable, given the large structural similarity between the two receptor types.

MR and GR are members of the nuclear receptor family, with a modular structure of an N-terminal domain, a DNA-binding domain (DBD) and C-terminal ligand-binding domain (LBD). Upon ligand binding, the receptors can dimerize and translocate to the nucleus, where they alter the transcription of their target genes. MR and GR can affect gene expression via tethering to other proteins such as AP-1 and NFκB (11), but in the hippocampus, at least under basal conditions, the main mechanism seems to be via direct DNA binding to the glucocorticoid response element (GRE), palindromic sequences that are variations of AGAACANNNTGTTCT (12). Homodimers as well as heterodimers of the receptors may occur (13, 14). The intrinsically unstructured N-terminal domain contains an Activator Function (AF)-1, and the LBD contains a ligand-dependent AF-2. Through these AF domains, the receptors can interact with coregulators, which can modulate the transcriptional effects by histone-modifying activity and recruitment/stabilization of the transcription factor complex (15). The fact that the two receptors are 94% identical in their DBD (16) suggests that other mechanisms must exist that confer transcriptional specificity underlying the differential effects of MR/GR.

It has remained elusive to what extent genomic targets of MR and GR overlap and what determines the specificity of MR and GR DNA binding. We previously identified genomic loci for GR, using chromatin immunoprecipitation-sequencing (ChIP-seq) after a single injection of corticosterone (12). In this study, we aimed to characterize mechanisms that confer MR/GR specificity by directly comparing their genomic binding sites in the same tissue. Our findings suggest that interactions between MR/GR and DNA-binding transcription factors from the NeuroD family are responsible for MR-selective signaling in the limbic brain and that NeuroD factors are able to potentiate transcriptional activity of both receptor types *in vitro*.

Material and Methods

In vivo experiment

For the ChIP-seq experiment, adult male Sprague-Dawley rats (Harlan, The Netherlands) were housed on a 12-hour light/12-hour dark cycle (lights on at 7:30 AM) with food and water *ad libitum*. ChIP-seq with MR, GR, or control immunoglobulin G (IgG) antibody was performed on hippocampal tissue of three-day adrenalectomized animals 60 minutes after a single intraperitoneal injection of 300 or 3000 μg/kg corticosterone as a 2-hydroxypropyl-β-cyclodextrin complex, as described (12). ChIP-seq was done on pooled tissue from six animals per treatment, which was redivided, leading to four technical ChIP replicates for both MR and GR. All experiments were performed according to the European Commission Council Directive 2010/63/EU and the Dutch law on animal experiments and approved by the animal ethical committee from Leiden University.

ChIP-seq analysis and motif search

The MR binding data were generated and analyzed in parallel with the previously published data for GR (12). Illumina Genome Analyzer 35-bp single-end reads were uniquely mapped to the rattus norvegicus genome version 4. Peaks were called using model-based analysis of ChIP-Seq (MACS) (17) with the IgG antibody binding dataset as the background. Binding sites were considered overlapping if more than 4 bp were shared. Data were visualized by uploading wiggle files to the Integrative Genomics Viewer (18). Using the annotate peak function of HOMER, binding sites were associated to their nearest gene (19). The Database for Annotation, Visualization, and Integrated Discovery was used for gene ontology analysis (20). Binding sequences were analyzed for the presence of *de novo* motifs using multiple expectation maximization for motif elicitation (21). The motif size was set from 6 bp minimum to 20 bp maximum, searching also the reverse complement, with a maximum of 10 output motifs, using random, shuffled input sequences as the background model. Enriched motifs were compared against the JASPAR vertebrate database of known motifs using the TOMTOM motif comparison tool. Analysis of Motif Enrichment (AME) was used for enrichment analysis of known motifs in MR-exclusive relative to GR-exclusive binding sequences, and Motif Alignment and Search Tool (MAST) was used for directed search of motifs of interest, under default settings (21).

ChIP-qPCR validation

For binding site validation, we performed ChIP-quantitative polymerase chain reaction (qPCR) on hippocampal tissue of intact rats killed at the time of their endogenous corticosterone peak. Antibodies used are listed in Supplemental Table 1. Protease inhibitors (Roche) were added to all buffers during tissue processing and the ChIP procedure. Hippocampal hemispheres were fixated with 1% formaldehyde for 12 to 14 minutes and were homogenized in Jiang buffer [0.32 M sucrose, 5 mM $CaCl_2$, 3 mM $Mg(Ac)_2$, 0.1 mM EDTA, 10 mM tris (hydroxymethyl)aminomethane-HCl, pH 8.0, 0.1% Nonidet P (NP)-40] using a glass douncer (Kimble-Chase). The following steps were performed in NP buffer [150 mM NaCl, 50 mM tris (hydroxymethyl)aminomethane-HCl, pH 7.5, 5 mM EDTA, 0.5% NP-40, 1% Triton X-100]. Chromatin was fragmented by sonication for 32 minutes with 30-second ON/30-second OFF cycles, using a Bioruptor Pico (Diagenode). Three processed hippocampal hemispheres were pooled and redivided to perform a ChIP for both MR and Neurod2. From each chromatin sample, an aliquot was taken as input material to be able to calculate the percentage of immunoprecipitated DNA.

Chromatin (500 μL) was incubated overnight with 6 μg antibody, after which 20 μL protein A Sepharose beads (GE Healthcare) was added for 2.5 hours. After several washing steps (Supplemental Methods), antibody-bound DNA was eluted from the beads using 10% Chelex 100 (Bio-Rad), further purified by phenolization and dissolved in 50 μL H_2O. qPCR was performed on 4x diluted ChIP samples according to the protocol described below. Primers were designed to span the GRE of the discovered binding sites and are listed in Supplemental Table 2.

Reporter assays

For mechanistic insights into the effect of NeuroD factors on MR/GR promoter activity, we performed luciferase reporter assays. HEK293 cells (human embryonic kidney, female) were cultured in Dulbecco's Modified Eagle Medium with GlutaMax (Gibco) containing 100 U/mL penicillin, 100 μg/mL streptomycin (Gibco) and 10% fetal bovine serum (PAN-Biotech) at 37°C under 5% CO_2. For the reporter assays, cells were seeded in a 24-well plate at a density of 80,000 cells/well and grown in medium supplemented with charcoal-stripped fetal bovine serum (Sigma) to exclude cortisol action from the serum. Cells were transfected on day 2 with luciferase construct (TAT1-Luc or TAT3-Luc: 25 ng/well; GRE-At, MRE-At, or GRE-MutAt: 30 ng/well), expression vector for one of the receptors (MMM, ΔMM, MMΔ, GGG, ΔGG, GGΔ: 10 ng/well), and pCMV-Myc-Neurod1/2/6 (0-1-3-10-50-100 ng/well) and completed with pcDNA3.1 to a total of 300 ng/well and 1.25 μL/well FuGENE (Promega) in unsupplemented Dulbecco's Modified Eagle Medium. Renilla luciferase was used to correct for transfection efficiency (1 ng/well, pRL-CMV; Promega). On day 3, cells were stimulated with corticosterone (10^{-7} M or at indicated concentrations; Sigma) dissolved in ethanol, and diluted in medium with a final concentration of 0.1% ethanol. After 24 hours, the cells were washed with phosphate-buffered saline, and reporter protein was measured using the Dual-Luciferase Reporter Assay System according to the manufacturer's instruction (Promega). Briefly, 100 μL lysis buffer was added, and after 10 minutes, 10 μL lysate was transferred into a half-area 96-well plate. Luciferase levels were quantified with 25 μL luciferase assay substrate at 570 nm; subsequently, Renilla signal was measured at 470 nm after the addition of 25 μL Stop and Glo at a SpectraMax L microplate reader (Molecular Devices). All data are presented as mean ± standard error of the mean. Reporter assays were done in triplicates and repeated at least once.

Plasmids

The GRE-At and GRE-MutAt luciferase constructs were created by inserting a 36-bp fragment containing a perfect palindromic GRE plus the Atoh1 motif or the GRE with a scrambled motif in the XhoI site of a pGL4.10[luc2] vector (Promega). Inserts were GRE-At: ctcgagGATGGCAGATGGAGCTAAGAACAGAATGTTCTATAActcgag and GRE-MutAt: ctcgagGATGGAGCGGATAGCTAAGAACAGAATGTTCTATAActcgag. The MRE-At luciferase construct was created by inserting a 35-bp endogenously found MR binding site containing a more degenerate GRE plus the Atoh1 motif in the *Nhe*I/*Bgl*II site of the same pGL4 vector. MRE-At insert was: gctagcGCACACAGATGAGTGGGGATCTGAATGTACTGTGGagatct. The pCMV-Myc-Neurod6 expression vector was kindly provided by Dr. Mitsuhiko Yamada (22). *Neurod1* and *Neurod2* were amplified from Sprague-Dawley rat hippocampal complementary DNA (cDNA) using the primers forward 5′-CAGTAGTCGACCATGACCAAATCATACAGCGAG-3′, reverse 5′-GTACTCTCGAGTGCCTCTAATCGTGAAAGATGG-3′ and forward 5′-CAGTAGTCGACCATGCTGACCCGCCTGTT-3′, reverse 5′-GTACTCTCGAGAGGTCTCAGTTATGGAAAAACGC-3′, respectively, and cloned in frame into the *Sal*I/*Xho*I site of the same pCMV-Myc vector to gain pCMV-Myc-Neurod1 and pCMV-Myc-Neurod2. Expression vectors for rat receptors 6RMR (MMM), 6RGR (GGG), and their corresponding truncated receptors 6RMR/596C (ΔMM), 6RMR/N689 (MMΔ), 6RGR/407C (ΔGG), 6RGR/N525 (GGΔ), and TAT1/3-Luc reporters were kindly provided by Dr. David Pearce (23).

Real-time qPCR

To validate the NeuroD factor expression in the rat brain, we performed reverse transcription (RT)-qPCR measurements on Sprague Dawley tissue. Hippocampal hemispheres were homogenized in TriPure (Roche) by shaking the tissue with 1.0-mm-diameter glass beads for 20 seconds at 6.5 m/s in a FastPrep-24 5G instrument (MP Biomedicals). Total RNA was isolated with chloroform, precipitated with isopropanol, washed with 75% ethanol, and resuspended in nuclease-free H_2O. The purity and concentration of the RNA samples were measured on a NanoDrop 1000 spectrophotometer (Thermo Scientific). cDNA was reverse transcribed from 1 μg RNA using random hexamers and M-MLV reverse transcription (Promega) and incubated for 10 minutes at 25°C, 50 minutes at 45°C, and 10 minutes at 70°C. RT-qPCR was performed in duplo on 10× diluted cDNA (5 ng/μL) with final primer concentrations of 0.5 μM using GoTaq qPCR master mix (Promega) in a CFX96 real-time PCR machine (Bio-Rad). The program consisted of 40 cycles of 10 seconds at 95°C and 30 seconds at 60°C, followed by a melting curve generation from 65°C to 95°C in steps of 0.5°C. Primer sequences are listed in Supplemental Table 2.

Allen Brain Atlas correlations

Lists of MR-exclusive, MR-GR overlapping, and GR-exclusive genes corresponding to the intragenic and distal promoter (up to –5000 bp) ChIP-seq binding sites were evaluated for their coexpression with each studied NeuroD factor, using the mouse brain gene expression data from the Allen Brain Atlas (24). Pearson's correlation coefficient was used as a measure of similarity between the expression profile of the seed genes (*Neurod1*, *Neurod2*, and *Neurod6*) and every gene in the three aforementioned lists within an anatomical region of interest (25). Correlations were calculated in the hippocampus and its subregions cornu ammonis (CA)1 to CA3 and the dentate gyrus (DG) as well as the striatum. To assess the strength of the association between each gene list and a seed gene, we used a one-sided Wilcoxon rank-sum test.

Data deposition

ChIP-seq data have been submitted to the European Nucleotide Archive and will be available under accession number PRJEB18916.

Results

MR-GR binding site overlap

ChIP-seq on hippocampus chromatin with MR and GR antibodies resulted in the generation of 1.3 to 1.9 × 10^7 reads per sample. After uniquely mapping 66.6% to 83.5% of these reads to the rat genome (rattus norvegicus genome version 4), MACS peak calling with a false discovery rate cutoff at 13.5% [conform (12); Supplemental Fig. 1(a)] resulted in 768 MR sites in the animals injected with 300 μg/kg (MR300) and 1465 MR sites and 2460 GR sites in the animals injected with 3000 μg/kg (MR3000 and GR3000).

We computed the overlap in binding-site genomic coordinates for MR and GR [Fig. 1(a)]. Additional filtering of MR- and GR-exclusive sites demanded total absence of any peak (the MACS lists including those peaks with a false discovery rate above 13.5%) at the same locus in the GR and MR data, respectively. This resulted in 918 MR-exclusive sites (combined from the MR300 and MR3000 dataset), 475 MR-GR overlapping sites, and 1450 GR-exclusive sites (Supplemental Table 3). These correspond to 45.9% of the total MR sites and 58.9% of the total GR sites being nonoverlapping. ChIP-seq traces of an MR-exclusive, MR-GR overlapping, and GR-exclusive peak are shown in Supplemental Figure 2. The distribution of sites relative to nearest genes is similar for these subsets, with approximately 40% to 45% of the binding sites located within promoters and genes, mainly in introns [Supplemental Fig. 1(b)]. Limited overlap was found between the MR binding sites for the two different dosages, as only 30.6% of the MR300 sites were also found in the MR3000 dataset.

Validation of MR binding sites

The GR binding sites were thoroughly validated before (12). We performed ChIP-qPCR measurements for MR in the hippocampus of intact animals killed at the time of their endogenous corticosterone peak. MR binding was detected at all tested MR-exclusive sites, whereas no MR signal was found at any of the GR-exclusive sites [Fig. 2(a)]. This demonstrates that the selectivity found in the pharmacological ChIP-seq experiment also occurs in a physiological context.

Processes associated with MR and GR target genes

The biological relevance of the hippocampal binding sites was examined by gene ontology enrichment analysis of target genes, under the assumption that expression of MR/GR bound genes will be regulated by the receptor. Intragenic and upstream (up to –5 kb) binding sites were annotated to generate lists of MR-exclusive, overlapping, and GR-exclusive target genes (Supplemental Table 4). Functional annotation clustering using the Database for Annotation, Visualization, and Integrated Discovery showed enrichment of brain-related terms, such as "Regulation of cell projection assembly" (MR), "Synapse, Regulation of synaptic plasticity" (overlapping), and "Cell/neuron projection, Synaptic vesicle" (GR) (Supplemental Table 5). Interestingly, for those genes linked to specific MR binding, there was enrichment for "Sodium channel activity," "Calcium ion transport," and "Ion transport, voltage-gated channel activity." Another term specific for MR-exclusive target genes was "Cell adhesion." Furthermore, the annotated GR-exclusive target genes were associated with "Apoptosis and Response to oxidative stress."

An additional motif was found near MR-exclusive sites

To explore the biological mechanism underlying MR/GR-selective binding, we performed *de novo* motif analysis on the binding site sequences. For the MR as well as the overlapping and GR datasets, all sites contained a GRE [Fig. 1(b)]. This is in contrast to the aldosterone-induced MR cistrome in a human renal cell line, where the majority of binding sites lack a GRE (26). The MR-exclusive sites had a more degenerate GRE (lower probability of bases) than the GR-exclusive sites. All subsets also contained a motif that matched the ZNF263 binding site, which was present in 18% to 67% of the sequences. The MR-GR overlapping sites all contained a motif that resembles a GRE half site, suggestive of concomitant dimeric and monomeric (or multimeric) binding of the receptors.

Interestingly, we found a distinct motif near the MR-exclusive sites that was not enriched near the GR-exclusive or overlapping sites. This additional motif was present in 100% of the MR sites and matched to the Atoh1 binding sequence in the motif database. In a directed search, the Atoh1 motif was also enriched in MR over GR binding (AME; $P = 1.11 \times 10^{-24}$), although in individual cases, we observed this site near GR-bound GREs (MAST; 1% of the GR-exclusive sites). The distance between the GRE and Atoh motif was normally distributed [Fig. 1(c)] and independent of their respective orientation/strand (in or out of phase) or the binding site relative to genes (intergenic vs intragenic) [Supplemental Fig. 1(c)]. We supposed that another protein binding to this Atoh site can drive MR-specific binding.

NeuroD family members as candidate binders

According to the Allen Brain Atlas (24), *Atoh1* is not expressed in the mouse hippocampus (Fig. 3; Table 1) and is therefore not considered a candidate to bind the MR-specific motif found in the hippocampal ChIP-seq dataset.

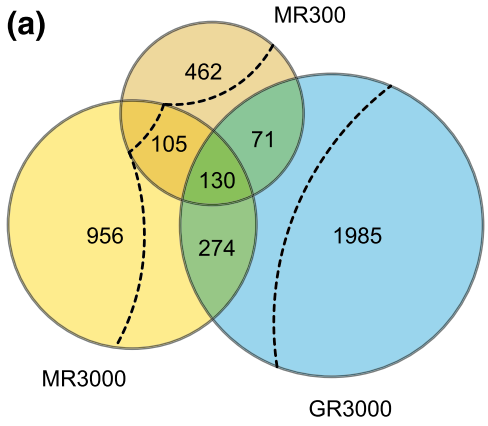

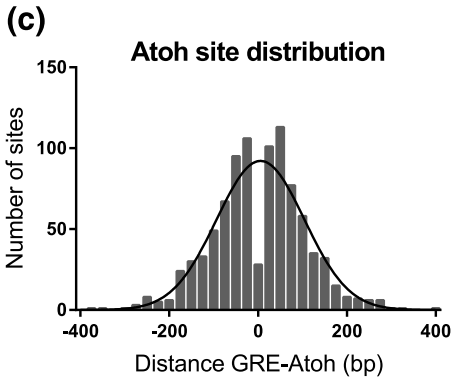

(b)

MR-exclusive (918 sites)	E-value	Matching TF
100%	1.4e-271	NR3C1 (GRE) 3.5e-06
100%	2.5e-163	Atoh1 5.2e-03
4%	3.0e-104	EGR2 1.0e-02
18%	1.2e-024	ZNF263 1.0e-02
6%	1.4e-007	Zfp281 4.5e-04

Overlapping (475 sites)	E-value	Matching TF
100%	3.8e-400	NR3C1 (GRE) 2.4e-07
67%	6.0e-075	ZNF263 6.2e-07
100%	5.6e-034	NR3C1 (*GRE half site?*) 1.9e-02
3%	1.9e-033	EGR2 6.4e-03

GR-exclusive (1450 sites)	E-value	Matching TF
100%	2.7e-1201	NR3C1 (GRE) 3.3e-12
37%	5.5e-114	-
3%	6.8e-103	EGR2 8.1e-03
23%	7.5e-078	ZNF263 5.8e-05

Figure 1. ChIP-seq binding site analysis. (a) Overlap of MR and GR binding sites in the rat hippocampus, from animals injected with 300 μg/kg (MR300) or 3000 μg/kg (MR3000 and GR3000) corticosterone. Dashed lines represent the additional filtering of nonoverlapping sites demanding total absence of any peaks in the other receptor dataset, leading to 918 MR-exclusive (combined from MR300 and MR3000), 475 overlapping, and 1450 GR-exclusive sites. (b) *De novo* motif analysis of MR-exclusive, overlapping, and GR-exclusive binding sites. Discovered motifs are depicted with their E-value (multiple expectation maximization for motif elicitation) and the highest-ranked matching transcription factor (TF). Listed transcription factors are followed by the E-value (TOMTOM) for the motif comparison. (c) Distribution of distance between GRE and Atoh motifs over 25-bp bins, including a normal curve. Depletion of the histogram bin around zero is due to the minimum distance of 8 bp as calculated from the center of the GRE to the center of the Atoh motif.

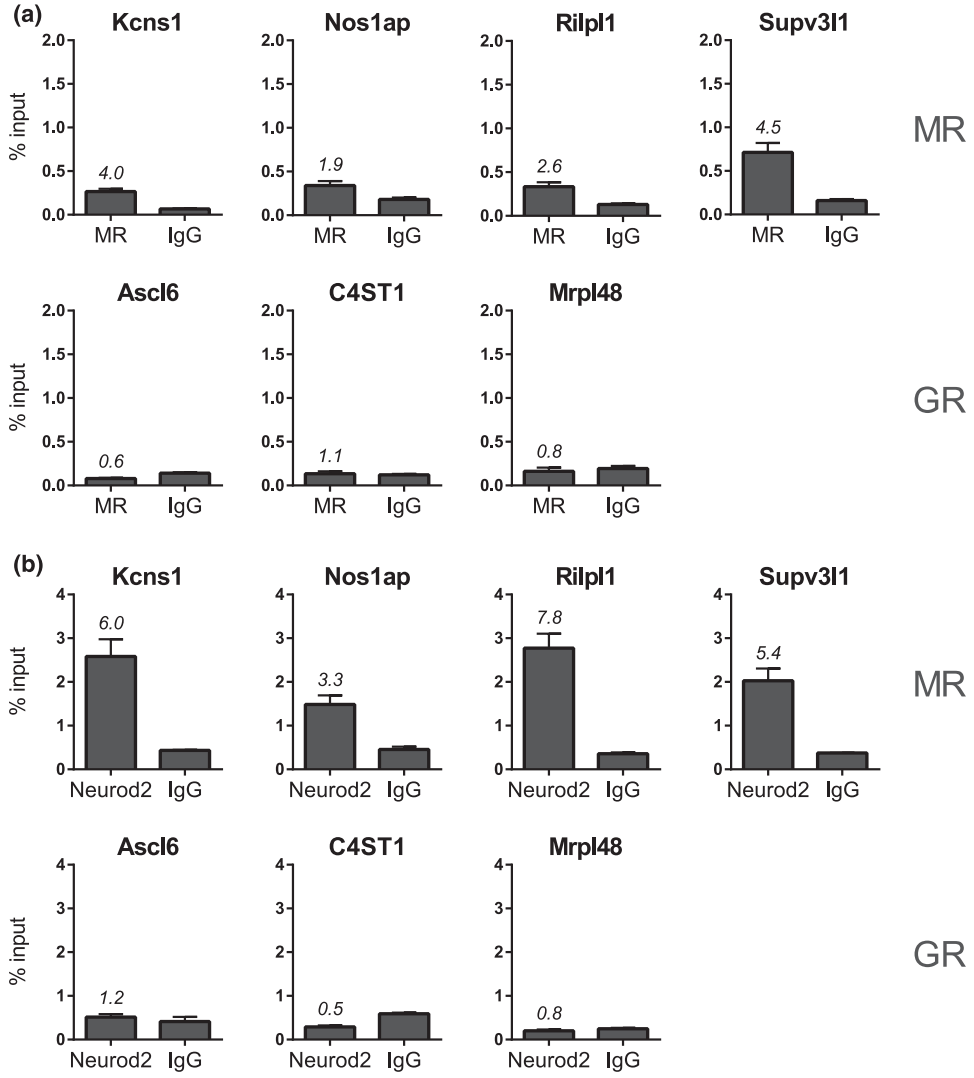

Figure 2. ChIP-qPCR validation of (a) MR (n = 5) and (b) Neurod2 (n = 6) binding to a subset of MR-exclusive and GR-exclusive binding sites. Numbers indicate the fold induction over IgG background.

Atoh1 belongs to the basic helix-loop-helix (bHLH) family of transcription factors (27). Brain-specific family members *Neurod1*, *Neurod2*, and *Neurod6* do show evident hippocampal expression (Fig. 3) and have been shown to bind the identified CAGATGG motif (28–30). We validated the very low expression levels (or absence) of *Atoh1* and expression of the three NeuroD genes in the rat hippocampus by RT-qPCR (Table 1) and hypothesized (one of) these corresponding proteins could be responsible for the binding site selectivity for MR.

By ChIP-qPCR, we demonstrated Neurod2 binding at the same sites at which we validated MR binding [Fig. 2(b)]. It was however absent from GR-exclusive loci. This gives a proof of concept that Neurod2 might be binding to the Atoh site *in vivo*. Although Neurod2 was selected based on the availability of chromatin immunoprecipitation–grade antibodies, this result does not exclude involvement of Neurod1 or Neurod6 in MR-selective signaling.

In vivo coexpression of NeuroD factors with putative MR/GR target genes

To get an indication if the other two NeuroD factors could be (co)responsible for the MR-selective binding *in vivo*, we examined to what extent they are coexpressed with putative MR/GR target genes (as defined by intragenic or up to –5-kb binding of MR or GR). We assessed the spatial coexpression of the MR, overlapping, and GR target gene lists with each of the NeuroD family members based on their expression patterns across the brain using data from the Allen Brain Atlas (24). The MR targets had a stronger coexpression with *Neurod6* than the overlapping or GR targets, while for *Neurod2*, there was no difference between the three lists, and the *Neurod1* spatial correlation was highest for the GR targets (Supplemental Fig. 3). This could argue for Neurod6 as an *in vivo* determinant of MR-selective signaling. Nevertheless, all three NeuroD factors correlated strongly with the expression of MR-exclusive targets and were subsequently studied *in vitro*.

NeuroD family members potentiate MR/GR transactivation

The putative role of Neurod1, Neurod2, and Neurod6 in MR-specific signaling was further studied in reporter assays in HEK293 cells. All three proteins potentiated MR but unexpectedly also GR transactivation upon corticosterone treatment on a luciferase construct containing a GRE plus the additional Atoh motif in its promoter (GRE-At) by approximately fourfold and sevenfold to ninefold, respectively (Fig. 4). This effect was not observed at a control construct lacking the Atoh binding site (GRE-MutAt), and the NeuroDs could not enhance reporter expression without hormone stimulation. The NeuroD factors thus acted as MR/GR transcriptional coactivators via the identified Atoh motif. For

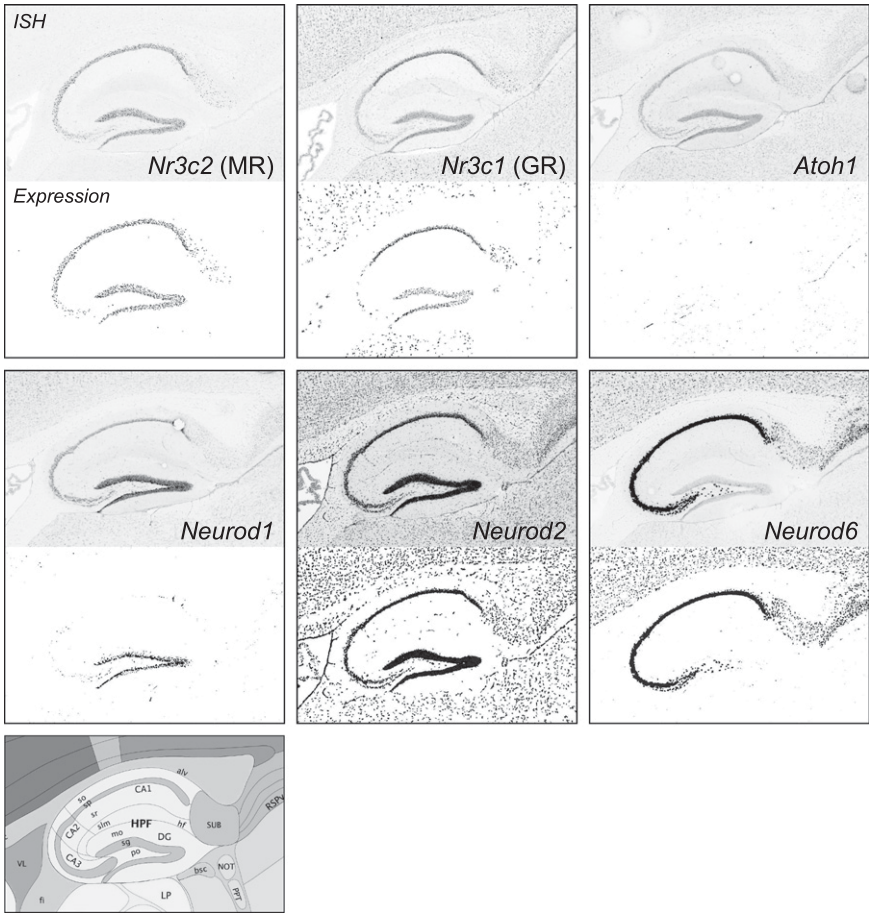

Figure 3. Expression of MR, GR, Atoh1, and NeuroD family members in the adult mouse hippocampus, with the corresponding reference atlas. Visualizations of the sagittal *in situ* hybridization (ISH) experiments and corresponding background-subtracted signals (Expression) from the Allen Brain Atlas (24). Experiment_position numbers of depicted images are listed in Supplemental Methods.

Neurod6, a clear dose- response curve was observed for transfection with increasing doses of expression vector [Supplemental Fig. 4(a)]. We further tested a reporter driven by a more degenerate GRE, as found for the MR-exclusive sites [Fig. 1(b)], combined with the additional Atoh site (MRE-At). The receptors were less efficient in stimulating this luciferase promoter, and the NeuroD effect also did not differ for MR and GR on this reporter [Supplemental Fig. 4(b)].

NeuroD family members increase mainly the maximum transcriptional effect

As the mechanism of action of a receptor modulator can be deduced from both the change in maximum effect as well as the ligand concentration needed for 50% of this effect (EC50) (31), we generated corticosterone dose-response curves with and without cotransfecting Neurod6. The maximum MR/GR effect was increased by Neurod6 presence over the whole concentration range that activates the receptor (data not shown), as was seen before by increased luciferase expression at saturating corticosterone concentrations of 10^{-7} M (Fig. 4). Besides, the EC50 was not changed for MR ($2.24 \pm 0.06 \times 10^{-10}$ M vs $1.89 \pm 0.05 \times 10^{-10}$ M), while the GR showed a slightly decreased EC50 upon Neurod6 addition ($1.03 \pm 0.05 \times 10^{-8}$ M vs $5.29 \pm 0.02 \times 10^{-9}$ M) [Fig. 5(a)].

NeuroD family members interact with both N- and C-terminal domain–lacking receptors

To further investigate the mechanism of interaction between the MR/GR and NeuroD factors, reporter assays were performed using truncated receptors [Fig. 5(b)]. The transactivation by receptors lacking the LBD (MMΔ and GGΔ) could be potentiated by the different NeuroDs, although to a lesser extent than for the full-length receptors (MMM and GGG). The potentiation by NeuroDs was also seen without hormone treatment of these constitutively active receptors lacking the LBD. Besides, the NeuroDs could also increase transcriptional activity of the receptors that did not have an N-terminal domain (ΔMM and ΔGG). For MR, the NeuroD potentiation of the truncate was comparable to that for the full-length receptor, but for GR, the enhancement relative to nonstimulated cells was less than one-half that of the full-length receptor. Unexpectedly, the ΔMM and ΔGG were unresponsive to corticosterone treatment at this reporter, but we did confirm proper transactivation at TAT1-Luc and TAT3-Luc reporters (data not shown). This potentiation of both N- and C-terminal receptor truncations suggests that NeuroD factors have an indirect interaction with MR/GR.

Discussion

This study examined the overlap and specificity of MR vs GR regarding whole-genome hippocampal binding sites. We found both MR-specific, GR-specific, and joint sites, which all contained a GRE. Virtually all MR-specific sites had an Atoh consensus sequence within 400 bp of the GRE, whereas *de novo* motif analysis did not find this sequence near sites that showed GR occupancy (including overlapping sites). Neurod1, Neurod2, and Neurod6 are coexpressed with MR and/or GR in the principal

Table 1. Overview of Atoh1 and NeuroD Family Members and Validation of mRNA Expression Levels in Rat Hippocampus

			Adult Hippocampal Expression		
Protein	**Synonyms**	**Expression Peak**	**Subregion**	**ABA (Mouse)**	**Ct (Rat)**
Atoh1	Hath1, Math1, bHLHa14	Early embryonic	—	0.24	>33.0
Neurod1	BETA2, BHF-1, Neurod, bHLHa3	E16-P0[a]	Both CA and DG (higher in DG)	1.41	23.2
Neurod2	Ndrf, bHLHa1	Stable throughout development[a]	Both CA and DG	10.41	22.0
Neurod3	Neurog1, AKA, Math4C, bHLHa6, Ngn1	Early embryonic	—	0.29	—
Neurod4	AI846749, ATH-3, Atoh3, Math3, bHLHa4	Early embryonic	—	0.12	—
Neurod5	Atoh6	—	—	—	—
Neurod6	Atoh2, Math2, Nex, Nex1m, bHLHa2	P5[a]	CA1–CA3	11.73	21.0

The effect of Neurod1, Neurod2, and Neurod6 on glucocorticoid signaling was studied *in vitro*. Raw expression value in adult mouse hippocampal formation, β-actin = 21.17; as a reference, MR = 0.68, GR = 2.18. The threshold cycle (Ct) values represent RT-qPCR measurements on 5 ng/μL cDNA, Sprague-Dawley rat whole hippocampus, β-actin = 17.8.

Abbreviations: ABA, Allen Brain Atlas.

[a]From ref. 50.

hippocampal cell layers, and all could act as coactivators of both MR and GR in reporter assays.

The limited overlap found in MR and GR binding sites is in accordance with the distinct roles of the two receptors in the hippocampus (6, 10, 32). It should be noted however that the lower sequencing depth of our analysis might have precluded the detection of weaker binding sites. In addition, as we performed ChIP-seq on whole hippocampi, the small proportion of shared targets could also be a result of cell type–specific MR/GR loci as a consequence of the differential MR and GR expression patterns throughout the hippocampal area. Coexpression of MR and GR is observed in the majority of CA pyramidal and DG granular neurons, with the exception of CA3 pyramidal cells that have high MR but low GR levels (33). Besides, GR is also expressed in glial cells (34, 35).

Limited overlap in the MR binding sites for the two different corticosterone doses (MR300 vs MR3000) could be explained partly by an insufficient depth of sequencing (limit of detection). In addition, it might reflect different concentrations of activated MR in the nucleus, in combination with differential affinity of binding sequences for the receptor, even if the majority of MR likely was occupied by the lower dose. A recent study suggests that high receptor occupancy does not necessarily translate into high DNA binding, and MR can show circadian variation in target site occupancy (36). Differences in sensitivity between MR-expressing cell types might also be of relevance. A last possibility may be opening up of chromatin domains via GR, making GREs available for MR binding. In the same line, heterodimerization of MR and GR could play a role (36).

The additional MR-selective motif could be bound by Neurod1, Neurod2, and Neurod6, as evidenced by response element–dependent transcriptional modulation. NeuroD proteins are members of the bHLH protein family and are known for their function in neuronal differentiation (28, 37). *Neurod1* knockout mice lack a dentate granule cell layer (38), and heterozygous *Neurod2*-deficient mice show impaired contextual and cued freezing in a fear-conditioning task (29). Our binding sites were detected in adult rat hippocampal tissue, suggesting that the NeuroD factors not only regulate neuronal differentiation during development, but also can be crucial in later processes such as cell survival or retaining differentiation status. As the hippocampal DG is the main site of adult neurogenesis (39), this might also provide a role for NeuroD factors in adulthood, although their expression is much wider than neurogenic zones. Furthermore, overexpression of Neurod2 in the ventral hippocampus has recently been shown to increase stress susceptibility in a chronic social defeat paradigm (40), posing a role for Neurod2 in depression.

Based on mouse brain expression data from the Allen Brain Atlas, we observed that *Neurod6* expression is restricted to the CA subregions of the hippocampus, while the lower *Neurod1* signal seems to be more pronounced in the DG (Fig. 3). Furthermore, *Neurod2* expression is observed throughout the whole hippocampus

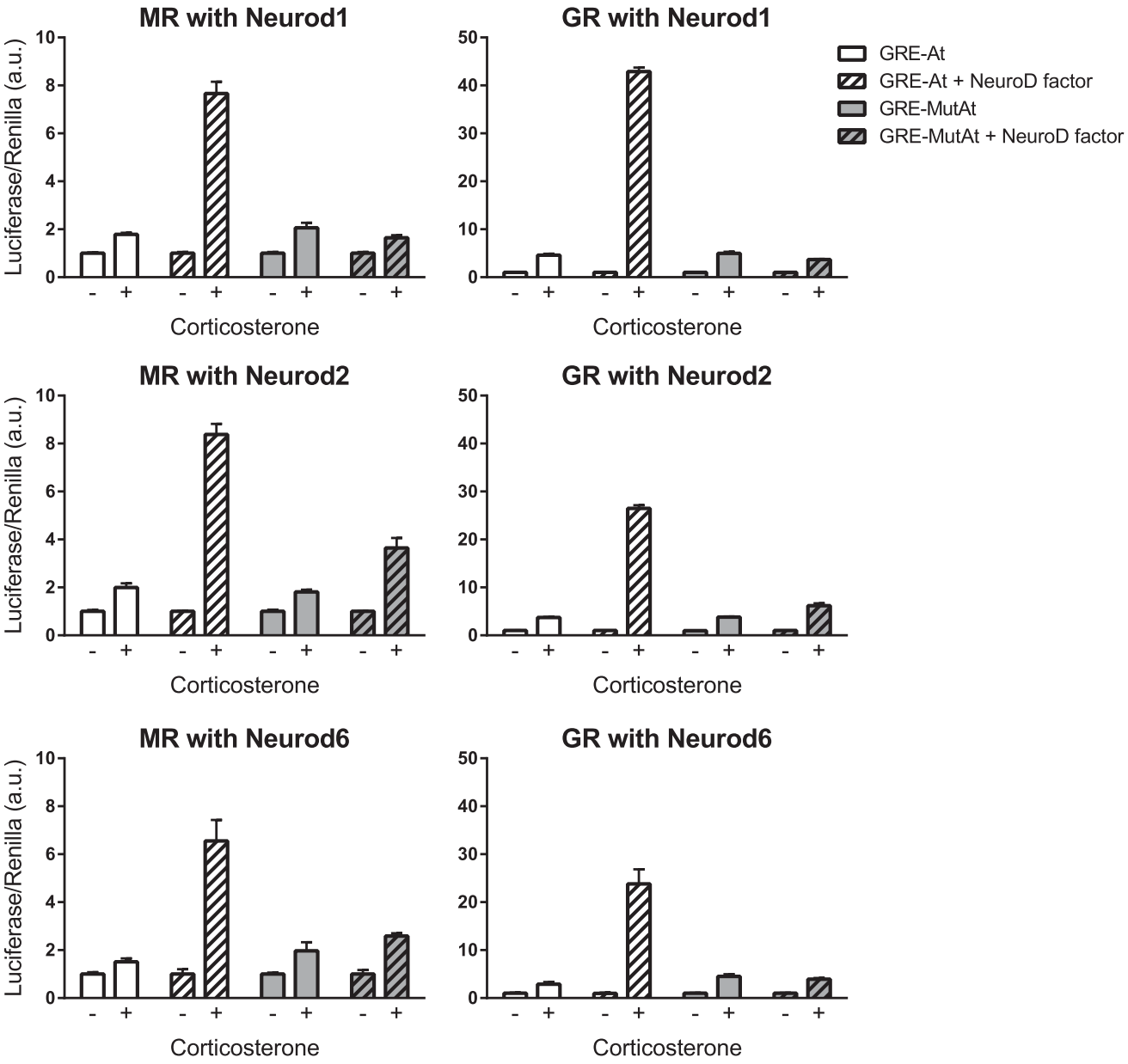

Figure 4. Potentiation of MR and GR transactivation by NeuroD family members on a luciferase construct containing a perfect GRE plus the additional MR-exclusive motif. HEK293 cells were transfected with MR or GR, the GRE-At or GRE-MutAt luciferase constructs, and Neurod1, Neurod2, or Neurod6 (10 ng/well) and stimulated with corticosterone (10^{-7} M). Nonstimulated cells were normalized to 1. a.u., arbitrary unit.

and seems to be at levels similar to *Neurod6*, as we validated by RT-qPCR on rat hippocampal tissue. The three NeuroD proteins have a highly similar bHLH region (37), which makes it not surprising that all members can bind the additional Atoh motif derived from our ChIP-seq analysis and potentiate MR/GR transactivation in reporter assays. Based on our data, we cannot pinpoint which of the family members is/are responsible for the MR-specific binding, although Neurod2 was detected at rat hippocampal MR-exclusive sites [Fig. 2(b)] and target gene correlations suggest that Neurod6 is also a likely candidate (Supplemental Fig. 3). We cannot exclude the possibility that another bHLH-containing protein binds to the Atoh motif and drives the exclusive MR action. *Neurod1*- or *Neurod2*-deficient mice that also lack *Neurod6* have more severe brain abnormalities than the single mutants, indicating cooperation and/or partial redundancy (41, 42). A model in which Neurod1, Neurod2, and Neurod6 are each involved in MR-specific signaling within a certain subregion of the hippocampus might be considered.

The *in vivo*-found, MR-exclusive motif does not discriminate *in vitro* in reporter assays. This discrepancy could be explained by the possibility that, in the luciferase assay, the receptors use different intermediate transcriptional proteins than in the hippocampus. The observed coactivation of both N- and C-terminally truncated receptors implies that NeuroD family members

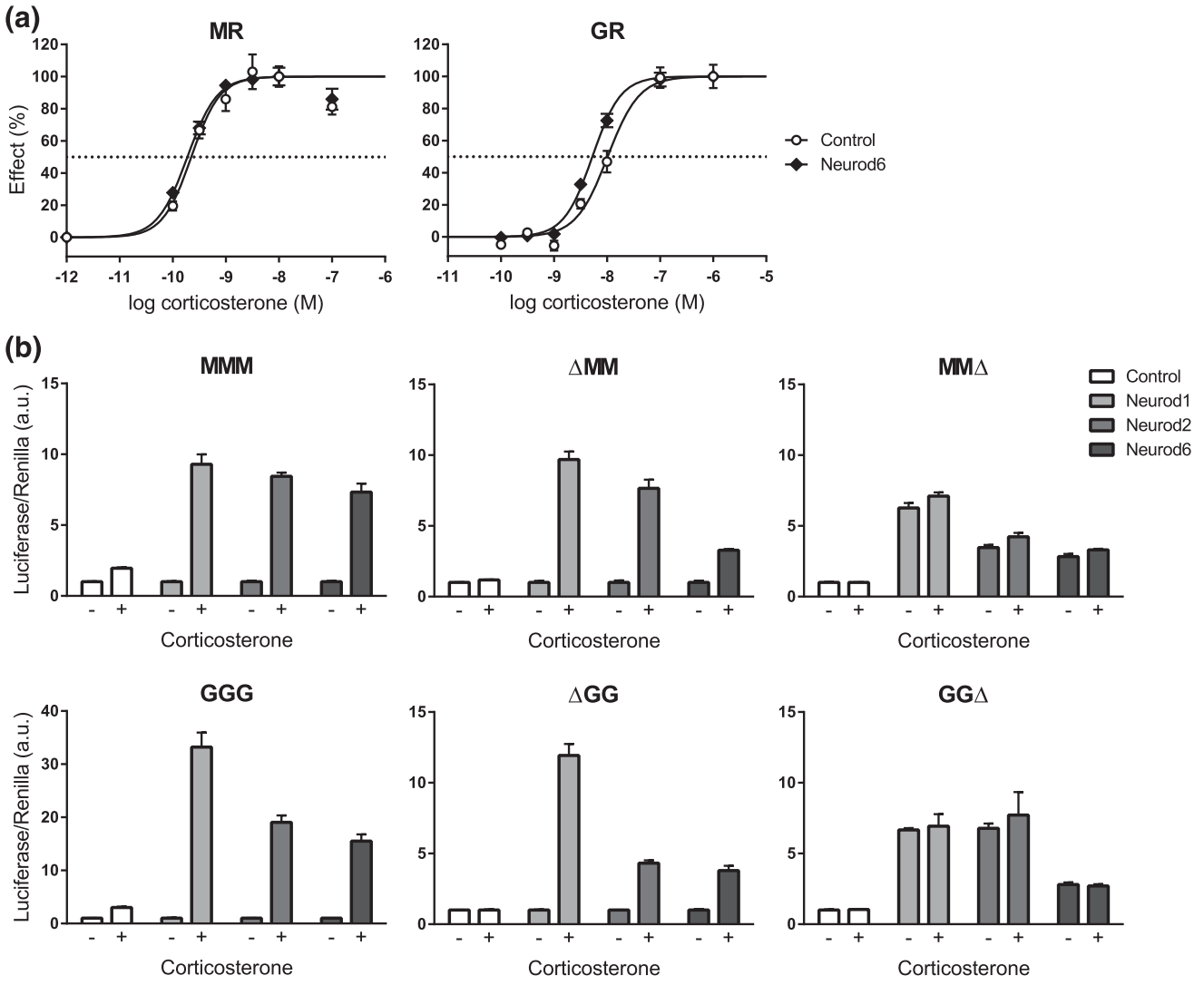

Figure 5. NeuroD increases the maximum MR/GR effect via an indirect mechanism of action. (a) Dose-response curves for corticosterone stimulation of MR and GR in absence and presence of Neurod6 to determine the effect on EC50. The luciferase activity is presented as percentage of the maximum effect. Sigmoidal curves were fit by nonlinear regression using a variable slope model. (b) Effect of NeuroD factors on truncated receptors. HEK293 cells were transfected with full MR or GR (MMM, GGG) or variants lacking the N terminus (ΔMM, ΔGG) or C terminus (MMΔ, GGΔ), the GRE-At construct, and Neurod1, Neurod2, or Neurod6 (10 ng/well) and stimulated with corticosterone (10^{-7} M). All nonstimulated cells were normalized to 1; for the constitutively active MMΔ and GGΔ, luciferase levels were normalized to nonstimulated control cells. a.u., arbitrary unit.

interact via the transcriptional complex of MR/GR rather than directly with the receptors. A side note is that we cannot rule out interactions via the DBD or hinge region of the receptors. Nevertheless, the suggested indirect interaction is also supported by the fact that the Atoh motif was found at a variable distance up to 400 bp from the GRE. It is likely that the HEK293 cells lack or do contain other variants of the proteins that are crucial to mediate the NeuroD effect on selective MR transcriptional activity. For example, the pool of coregulators present in a cell is highly tissue specific and can result in opposite effects on gene transcription (43). Also, bHLH protein heterodimerization partners might be responsible for an MR-specific effect (27). Besides, as the chromatin landscape is a crucial determinant of a transcription factor cistrome (44), the lack of chromatin context in the luciferase assay might make it difficult to mimic the exact conditions of *in vivo* binding and transcription. Interestingly, Neurod1 itself can also induce chromatin remodeling and increase neuronal gene accessibility (45).

In lung fibroblasts, the Atoh1 motif was detected, although nonsignificantly, near GR-bound sequences (46). Directed motif search by MAST showed the presence of a Neurod2 binding site in 1% of our GR-exclusive sites, but the Atoh motif was clearly enriched in MR-exclusive over GR-exclusive sites using AME. It might be that a NeuroD factor through binding to the Atoh motif only excludes GR binding and subsequent transactivation when MR is present, which can be another reason that we do not find a difference in MR/GR

potentiation *in vitro* when studying the receptors in isolation. In cotransfections of MR and GR combined with selective pharmacological activation, both receptors were also potentiated by Neurod6 (data not shown). Furthermore, the highly dynamic DNA-binding kinetics of nuclear receptors are not supportive of a competition-based mechanism (47, 48). A recent study also found motifs that were associated with absence of GR binding, and proteins recognizing these sequences could indeed decrease GR occupancy and transactivation (49).

In conclusion, we identified a motif that is associated with MR-selective signaling in the rat hippocampus. NeuroD factors could bind this motif and, via indirect interactions, were found to potentiate the MR/GR transcriptional activity in HEK293 cells. The data support a model in which NeuroD factors stabilize MR binding *in vivo* by interacting with cell-specific components of the MR-associated transcriptional complex. Further elucidation of distinct MR/GR downstream pathways will enable us to more specifically target aspects of glucocorticoid signaling for treatment of stress-related disorders.

Acknowledgments

We thank Robin Schoonderwoerd for technical assistance and Dr. Mitsuhiko Yamada and Dr. David Pearce for providing plasmids.

Address all correspondence and requests for reprints to: Lisa T.C.M. van Weert, MSc, Department of Medicine, Division of Endocrinology, Leiden University Medical Center, 2300 RC Leiden, The Netherlands. E-mail: l.t.c.m.van_weert@lumc.nl.

This work was supported by the Netherlands Organisation for Scientific Research (NWO) ALW Grant 823.02.002 and COST Action ADMIRE BM1301.

Disclosure Summary: The authors have nothing to disclose.

References

1. de Kloet ER, Joëls M, Holsboer F. Stress and the brain: from adaptation to disease. *Nat Rev Neurosci*. 2005;**6**(6):463–475.
2. Reul JM, de Kloet ER. Two receptor systems for corticosterone in rat brain: microdistribution and differential occupation. *Endocrinology*. 1985;**117**(6):2505–2511.
3. de Kloet ER, Otte C, Kumsta R, Kok L, Hillegers MH, Hasselmann H, Kliegel D, Joëls M. STRESS and DEPRESSION a crucial role of the mineralocorticoid receptor [published online ahead of print August 28, 2016]. *J Neuroendocrinol*. doi: 10.1111/jne.12379.
4. Joëls M, Karst H, DeRijk R, de Kloet ER. The coming out of the brain mineralocorticoid receptor. *Trends Neurosci*. 2008;**31**(1):1–7.
5. Vogel S, Fernández G, Joëls M, Schwabe L. Cognitive adaptation under stress: a case for the mineralocorticoid receptor. *Trends Cogn Sci*. 2016;**20**(3):192–203.
6. Oitzl MS, de Kloet ER. Selective corticosteroid antagonists modulate specific aspects of spatial orientation learning. *Behav Neurosci*. 1992;**106**(1):62–71.
7. Roozendaal B. Stress and memory: opposing effects of glucocorticoids on memory consolidation and memory retrieval. *Neurobiol Learn Mem*. 2002;**78**(3):578–595.
8. Sapolsky RM, Romero LM, Munck AU. How do glucocorticoids influence stress responses? Integrating permissive, suppressive, stimulatory, and preparative actions. *Endocr Rev*. 2000;**21**(1):55–89.
9. Joëls M, Sarabdjitsingh RA, Karst H. Unraveling the time domains of corticosteroid hormone influences on brain activity: rapid, slow, and chronic modes. *Pharmacol Rev*. 2012;**64**(4):901–938.
10. Joëls M, de Kloet ER. Mineralocorticoid receptor-mediated changes in membrane properties of rat CA1 pyramidal neurons in vitro. *Proc Natl Acad Sci USA*. 1990;**87**(12):4495–4498.
11. De Bosscher K, Vanden Berghe W, Haegeman G. The interplay between the glucocorticoid receptor and nuclear factor-kappaB or activator protein-1: molecular mechanisms for gene repression. *Endocr Rev*. 2003;**24**(4):488–522.
12. Polman JA, de Kloet ER, Datson NA. Two populations of glucocorticoid receptor-binding sites in the male rat hippocampal genome. *Endocrinology*. 2013;**154**(5):1832–1844.
13. Liu W, Wang J, Sauter NK, Pearce D. Steroid receptor heterodimerization demonstrated in vitro and in vivo. *Proc Natl Acad Sci USA*. 1995;**92**(26):12480–12484.
14. Trapp T, Holsboer F. Heterodimerization between mineralocorticoid and glucocorticoid receptors increases the functional diversity of corticosteroid action. *Trends Pharmacol Sci*. 1996;**17**(4):145–149.
15. Zalachoras I, Houtman R, Meijer OC. Understanding stress-effects in the brain via transcriptional signal transduction pathways. *Neuroscience*. 2013;**242**:97–109.
16. Arriza JL, Weinberger C, Cerelli G, Glaser TM, Handelin BL, Housman DE, Evans RM. Cloning of human mineralocorticoid receptor complementary DNA: structural and functional kinship with the glucocorticoid receptor. *Science*. 1987;**237**(4812):268–275.
17. Zhang Y, Liu T, Meyer CA, Eeckhoute J, Johnson DS, Bernstein BE, Nusbaum C, Myers RM, Brown M, Li W, Liu XS. Model-based analysis of ChIP-Seq (MACS). *Genome Biol*. 2008;**9**(9):R137.
18. Robinson JT, Thorvaldsdóttir H, Winckler W, Guttman M, Lander ES, Getz G, Mesirov JP. Integrative genomics viewer. *Nat Biotechnol*. 2011;**29**(1):24–26.
19. Heinz S, Benner C, Spann N, Bertolino E, Lin YC, Laslo P, Cheng JX, Murre C, Singh H, Glass CK. Simple combinations of lineage-determining transcription factors prime cis-regulatory elements required for macrophage and B cell identities. *Mol Cell*. 2010;**38**(4):576–589.
20. Huang W, Sherman BT, Lempicki RA. Systematic and integrative analysis of large gene lists using DAVID bioinformatics resources. *Nat Protoc*. 2008;**4**(1):44–57.
21. Bailey TL, Boden M, Buske FA, Frith M, Grant CE, Clementi L, Ren J, Li WW, Noble WS. MEME SUITE: tools for motif discovery and searching. *Nucleic Acids Res*. 2009;**37**(Web Server issue):W202–W208.
22. Yamada M, Shida Y, Takahashi K, Tanioka T, Nakano Y, Tobe T, Yamada M. Prg1 is regulated by the basic helix-loop-helix transcription factor Math2. *J Neurochem*. 2008;**106**(6):2375–2384.
23. Pearce D, Yamamoto KR. Mineralocorticoid and glucocorticoid receptor activities distinguished by nonreceptor factors at a composite response element. *Science*. 1993;**259**(5098):1161–1165.
24. Lein ES, Hawrylycz MJ, Ao N, Ayres M, Bensinger A, Bernard A, Boe AF, Boguski MS, Brockway KS, Byrnes EJ, Chen L, Chen L, Chen TM, Chin MC, Chong J, Crook BE, Czaplinska A, Dang CN, Datta S, Dee NR, Desaki AL, Desta T, Diep E, Dolbeare TA, Donelan MJ, Dong HW, Dougherty JG, Duncan BJ, Ebbert AJ, Eichele G, Estin LK, Faber C, Facer BA, Fields R, Fischer SR, Fliss TP, Frensley C, Gates SN, Glattfelder KJ, Halverson KR, Hart MR, Hohmann JG, Howell MP, Jeung DP, Johnson RA, Karr PT, Kawal R, Kidney JM, Knapik RH, Kuan CL, Lake JH, Laramee AR,

Larsen KD, Lau C, Lemon TA, Liang AJ, Liu Y, Luong LT, Michaels J, Morgan JJ, Morgan RJ, Mortrud MT, Mosqueda NF, Ng LL, Ng R, Orta GJ, Overly CC, Pak TH, Parry SE, Pathak SD, Pearson OC, Puchalski RB, Riley ZL, Rockett HR, Rowland SA, Royall JJ, Ruiz MJ, Sarno NR, Schaffnit K, Shapovalova NV, Sivisay T, Slaughterbeck CR, Smith SC, Smith KA, Smith BI, Sodt AJ, Stewart NN, Stumpf KR, Sunkin SM, Sutram M, Tam A, Teemer CD, Thaller C, Thompson CL, Varnam LR, Visel A, Whitlock RM, Wohnoutka PE, Wolkey CK, Wong VY, Wood M, Yaylaoglu MB, Young RC, Youngstrom BL, Yuan XF, Zhang B, Zwingman TA, Jones AR. Genome-wide atlas of gene expression in the adult mouse brain. *Nature*. 2006;**445**(7124):168–176.

25. Mahfouz A, Lelieveldt BP, Grefhorst A, van Weert LT, Mol IM, Sips HC, van den Heuvel JK, Datson NA, Visser JA, Reinders MJ, Meijer OC. Genome-wide coexpression of steroid receptors in the mouse brain: identifying signaling pathways and functionally coordinated regions. *Proc Natl Acad Sci USA*. 2016;**113**(10):2738–2743.
26. Le Billan F, Khan JA, Lamribet K, Viengchareun S, Bouligand J, Fagart J, Lombès M. Cistrome of the aldosterone-activated mineralocorticoid receptor in human renal cells. *FASEB J*. 2015;**29**(9):3977–3989.
27. Massari ME, Murre C. Helix-loop-helix proteins: regulators of transcription in eucaryotic organisms. *Mol Cell Biol*. 2000;**20**(2):429–440.
28. Fong AP, Yao Z, Zhong JW, Cao Y, Ruzzo WL, Gentleman RC, Tapscott SJ. Genetic and epigenetic determinants of neurogenesis and myogenesis. *Dev Cell*. 2012;**22**(4):721–735.
29. Lin CH, Hansen S, Wang Z, Storm DR, Tapscott SJ, Olson JM. The dosage of the neuroD2 transcription factor regulates amygdala development and emotional learning. *Proc Natl Acad Sci USA*. 2005;**102**(41):14877–14882.
30. Poulin G, Turgeon B, Drouin J. NeuroD1/beta2 contributes to cell-specific transcription of the proopiomelanocortin gene. *Mol Cell Biol*. 1997;**17**(11):6673–6682.
31. Simons SS Jr, Chow CC. The road less traveled: new views of steroid receptor action from the path of dose-response curves. *Mol Cell Endocrinol*. 2012;**348**(2):373–382.
32. Joëls M, De Kloet ER. Coordinative mineralocorticoid and glucocorticoid receptor-mediated control of responses to serotonin in rat hippocampus. *Neuroendocrinology*. 2008;**55**(3):344–350.
33. Van Eekelen JA, De Kloet ER. Co-localization of brain corticosteroid receptors in the rat hippocampus. *Prog Histochem Cytochem*. 1992;**26**(1-4):250–258.
34. Nichols NR, Osterburg HH, Masters JN, Millar SL, Finch CE. Messenger RNA for glial fibrillary acidic protein is decreased in rat brain following acute and chronic corticosterone treatment. *Brain Res Mol Brain Res*. 1990;**7**(1):1–7.
35. Vielkind U, Walencewicz A, Levine JM, Bohn MC. Type II glucocorticoid receptors are expressed in oligodendrocytes and astrocytes. *J Neurosci Res*. 1990;**27**(3):360–373.
36. Mifsud KR, Reul JM. Acute stress enhances heterodimerization and binding of corticosteroid receptors at glucocorticoid target genes in the hippocampus. *Proc Natl Acad Sci USA*. 2016;**113**(40):11336–11341.
37. Hassan BA, Bellen HJ. Doing the MATH: is the mouse a good model for fly development? *Genes Dev*. 2000;**14**(15):1852–1865.
38. Liu M, Pleasure SJ, Collins AE, Noebels JL, Naya FJ, Tsai MJ, Lowenstein DH. Loss of BETA2/NeuroD leads to malformation of the dentate gyrus and epilepsy. *Proc Natl Acad Sci USA*. 2000;**97**(2):865–870.
39. Fitzsimons CP, van Hooijdonk LW, Schouten M, Zalachoras I, Brinks V, Zheng T, Schouten TG, Saaltink DJ, Dijkmans T, Steindler DA, Verhaagen J, Verbeek FJ, Lucassen PJ, de Kloet ER, Meijer OC, Karst H, Joels M, Oitzl MS, Vreugdenhil E. Knockdown of the glucocorticoid receptor alters functional integration of newborn neurons in the adult hippocampus and impairs fear-motivated behavior. *Mol Psychiatry*. 2012;**18**(9):993–1005.
40. Bagot RC, Cates HM, Purushothaman I, Lorsch ZS, Walker DM, Wang J, Huang X, Schlüter OM, Maze I, Peña CJ, Heller EA, Issler O, Wang M, Song WM, Stein JL, Liu X, Doyle MA, Scobie KN, Sun HS, Neve RL, Geschwind D, Dong Y, Shen L, Zhang B, Nestler EJ. Circuit-wide transcriptional profiling reveals brain region-specific gene networks regulating depression susceptibility. *Neuron*. 2016;**90**(5):969–983.
41. Bormuth I, Yan K, Yonemasu T, Gummert M, Zhang M, Wichert S, Grishina O, Pieper A, Zhang W, Goebbels S, Tarabykin V, Nave KA, Schwab MH. Neuronal basic helix-loop-helix proteins Neurod2/6 regulate cortical commissure formation before midline interactions. *J Neurosci*. 2013;**33**(2):641–651.
42. Schwab MH, Bartholomae A, Heimrich B, Feldmeyer D, Druffel-Augustin S, Goebbels S, Naya FJ, Zhao S, Frotscher M, Tsai MJ, Nave KA. Neuronal basic helix-loop-helix proteins (NEX and BETA2/Neuro D) regulate terminal granule cell differentiation in the hippocampus. *J Neurosci*. 2000;**20**(10):3714–3724.
43. Lachize S, Apostolakis EM, van der Laan S, Tijssen AM, Xu J, de Kloet ER, Meijer OC. Steroid receptor coactivator-1 is necessary for regulation of corticotropin-releasing hormone by chronic stress and glucocorticoids. *Proc Natl Acad Sci USA*. 2009;**106**(19):8038–8042.
44. John S, Sabo PJ, Thurman RE, Sung MH, Biddie SC, Johnson TA, Hager GL, Stamatoyannopoulos JA. Chromatin accessibility predetermines glucocorticoid receptor binding patterns. *Nat Genet*. 2011;**43**(3):264–268.
45. Pataskar A, Jung J, Smialowski P, Noack F, Calegari F, Straub T, Tiwari VK. NeuroD1 reprograms chromatin and transcription factor landscapes to induce the neuronal program. *EMBO J*. 2015;**35**(1):24–45.
46. Starick SR, Ibn-Salem J, Jurk M, Hernandez C, Love MI, Chung HR, Vingron M, Thomas-Chollier M, Meijsing SH. ChIP-exo signal associated with DNA-binding motifs provides insight into the genomic binding of the glucocorticoid receptor and cooperating transcription factors. *Genome Res*. 2015;**25**(6):825–835.
47. Groeneweg FL, van Royen ME, Fenz S, Keizer VI, Geverts B, Prins J, de Kloet ER, Houtsmuller AB, Schmidt TS, Schaaf MJ. Quantitation of glucocorticoid receptor DNA-binding dynamics by single-molecule microscopy and FRAP. *PLoS One*. 2014;**9**(3):e90532.
48. Voss TC, Schiltz RL, Sung MH, Yen PM, Stamatoyannopoulos JA, Biddie SC, Johnson TA, Miranda TB, John S, Hager GL. Dynamic exchange at regulatory elements during chromatin remodeling underlies assisted loading mechanism. *Cell*. 2011;**146**(4):544–554.
49. Telorac J, Prykhozhij SV, Schöne S, Meierhofer D, Sauer S, Thomas-Chollier M, Meijsing SH. Identification and characterization of DNA sequences that prevent glucocorticoid receptor binding to nearby response elements. *Nucleic Acids Res*. 2016;**44**(13):6142–6156.
50. Schwab MH, Druffel-Augustin S, Gass P, Jung M, Klugmann M, Bartholomae A, Rossner MJ, Nave KA. Neuronal basic helix-loop-helix proteins (NEX, neuroD, NDRF): spatiotemporal expression and targeted disruption of the NEX gene in transgenic mice. *J Neurosci*. 1998;**18**(4):1408–1418.